## Supporting Information

# Revealing the Chemical Structure Dependent Carrier Trapping in One-Dimensional Antimony Selenide Photovoltaic Materials

Rui Cao,‡ Huiling Cai,‡ Weitao Lian, Rongfeng Tang, Yinan Xiang, Yan Wang and Tao Chen*

Institute of Energy, Hefei Comprehensive National Science Center, Hefei, China.

Department of Materials Science and Engineering, School of Chemistry and Materials Science, University of Science and Technology of China, Hefei, Anhui 230026, P. R. China. E-mail: tchenmse@ustc.edu.cn.

‡ These authors contributed equally to this work.

## Experimental Section

### Fabrication of $Sb_2Se_3$ films

$Sb_2Se_3$ films were fabricated on insulating substrate by thermal evaporation deposition method under a pressure of $5\times10^{-4}$ Pa. $Sb_2Se_3$ (99.99%, zhongnuoxincai) powder was utilized as thermal evaporation source, and suitable Sb (99.999%, Sinopharm) powder was co-evaporated to adjust the stoichiometry of $Sb_2Se_3$ films. We selected a suitable evaporated rate of around 5 nm $s^{-1}$ and obtained $Sb_2Se_3$ films around 300 nm. The substrate was preheated at 315 ºC. Eventually, $Sb_2Se_3$ films were annealed at 380 °C for 8 min in glove box filled with $N_2$.

### Fabrication of $Sb_2Se_3$ solar cells

The FTO glass (TEC-A7) was cleaned in the order of DI water, isopropanol, acetone, ethanol, then it was cleaned by UV ozone for 15 min. Afterwards, CdS electron transporting layer was deposited on as-cleaned FTO glass by CBD method. Then, $Sb_2Se_3$ film was deposited on CdS by thermal evaporation method. Afterwards, Spiro-OMeTAD was spin-coated on $Sb_2Se_3$ film as hole transport layer. Eventually, Au electrode was evaporated on the Spiro-OMeTAD layer under a pressure of $5\times10^{-4}$ Pa. The active area was defined as 0.04 $cm^{-2}$ by a metallic mask.

### Characterizations of films and devices

The crystallinity of $Sb_2Se_3$ films was characterized by XRD (Bruker Advance D8 diffractometer) with Cu K$\alpha$ radiation ($\lambda$ = 1.5406 Å). The SEM images of $Sb_2Se_3$ thin films were measured by FE-SEM (Hitachi SU8220) equipped with an EDS (Bruker) module. Raman spectroscopy (Horiba JobinYvon, LabRAM HR800) was measured to analyze chemical bonds of the films with 532-nm laser excitation. XPS results of the films were carried out with a monochromatic Al K$\alpha$ X-ray source to characterize the elemental composition of the surface by a Thermo Scientific K-Alpha+ instrument. UV-vis-NIR spectrophotometer (SOLID 3700) was used to measure the steady-state optical absorption of $Sb_2Se_3$ films. The *J-V* performance of $Sb_2Se_3$ films was measured by a Keithley 2400 equipment under solar-simulated AM 1.5G sunlight (a typical solar simulator based on xenon-lamp (Oriel Sol 3A)). Halogen lamp connected with monochromator (SPIEQ200) was as the single illuminated source to characterize the EQE of $Sb_2Se_3$ solar cells.

**Table S1.** The statistical chemical composition of $Sb_2Se_3$ films with 10 samples each for $Sb_2Se_3$, Se-rich and Sb-rich films probed by energy dispersive X-ray spectroscopy.

| **$Sb_2Se_3$ films** | **Se (at%)** | **Sb (at%)** | **Se/Sb** |
|---|---|---|---|
| Sb-rich | 58.40±0.92 | 41.60±0.92 | 1.41±0.05 |
| Se-rich | 60.95±0.35 | 39.05±0.35 | 1.56±0.02 |
| $Sb_2Se_3$ | 59.96±0.36 | 40.04±0.36 | 1.50±0.02 |

**Table S2.** Results of biexponential fitting of GSB decay.

| **$Sb_2Se_3$ films** | $A_1$ | $\tau_1$ **(ps)** | $A_2$ | $\tau_2$ **(ps)** | $\tau_{ave}$ **(ps)** |
|---|---|---|---|---|---|
| Sb-rich | -0.135 | 0.08 | -0.865 | 0.31 | 0.30 |
| Se-rich | -0.031 | 0.07 | -0.969 | 0.20 | 0.20 |

**Table S3.** Results of biexponential fitting that rely on Levenberg-Marquardt algorithm.

| **Sample** | $A_1$ | $\tau_1$ **(ps)** | $A_2$ | $\tau_2$ **(ps)** | $\tau_{ave}$ **(ps)** |
|---|---|---|---|---|---|
| Sb-rich $Sb_2Se_3$ | 0.115 | 14.6 | 0.649 | 3891.1 | 3888.5 |
| Se-rich $Sb_2Se_3$ | 0.128 | 20.2 | 0.703 | 4256.3 | 4252.7 |
| Sb-rich $Sb_2Se_3$ on CdS | 0.024 | 8.3 | 0.447 | 1972.7 | 1972.2 |
| Se-rich $Sb_2Se_3$ on CdS | 0.075 | 4.7 | 0.553 | 1410.7 | 1410.1 |

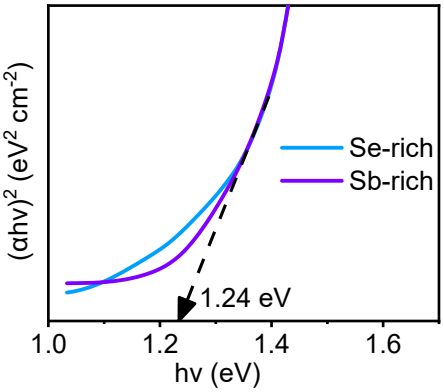


**Figure S1.** UV-vis spectroscopy of Sb-rich and Se-rich $Sb_2Se_3$ films.

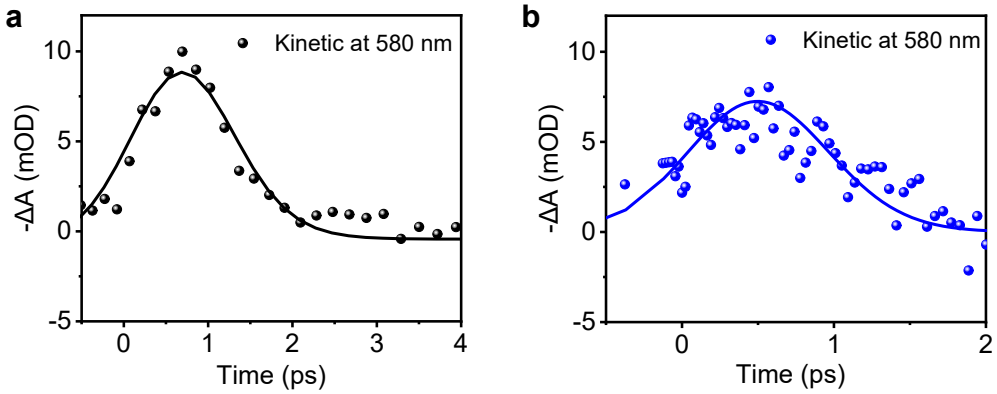


**Figure S2.** Transient kinetic traces of (a) Sb-rich $Sb_2Se_3$ films and (b) Se-rich $Sb_2Se_3$ films and their fits (solid lines).

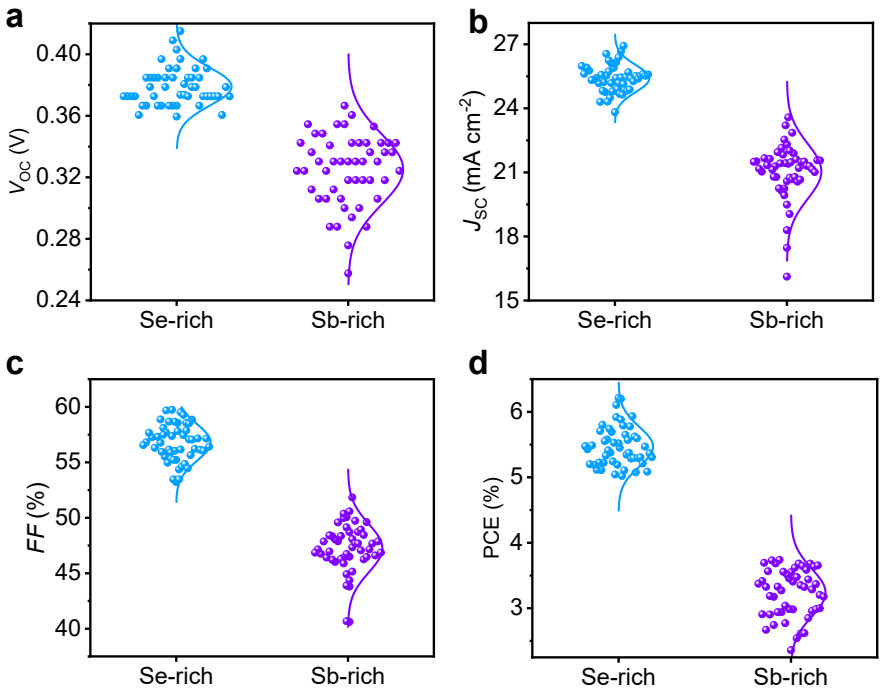


**Figure S3.** (a-d) Statistical $V_{OC}$, $J_{SC}$, *FF* and PCE of Se-rich and Sb-rich $Sb_2Se_3$ devices.

**Note S1.** TA characterization.

The carrier dynamics was obtained from femtosecond transient absorption spectroscopy (fs-TAS). The fs-TAS instrument we used comprises ultrafast laser system, light conversion, sample transport, delay generation and probe detection. Broad UV/vis probe band is achieved by generating continuous white light in different media (e.g., $CaF_2$, sapphire); the choice of media and seed energy determine the range of spectrum and shape of the generated continuous light.[1] Transient absorption (TA) measurements are performed on a pump-probe system (Helios, Ultrafast System) with the maximum delay time of ~8000 ps using a motorized optical delay line under ambient conditions. The pump pulses at 400 nm wavelength (~800 μW average power at the sample) are delivered by an ultrafast optical parametric amplifier (OPera Solo) excited by a regenerative amplifier (Coherent Astrella, 800 nm, 1 kHz), seeded with a mode-locked Ti:sapphire oscillator (Coherent Vitara, 800 nm, 80 MHz) and pumped with a LBO laser (Coherent Evolution-50C, 1 kHz system). A small amount of 800 nm femtosecond pulses from the regenerative amplifier are used to pump a sapphire crystal to create a 320-780 nm white light continuum as probe pulses. Interpulse fluctuations of continuous white light probe pulses are corrected using a self-splitting reference beam (Reference). The mechanical chopper operates at a frequency of 500 Hz and is used for modulating the pump pulses. The TA decay is fitted with biexponential function:

$$\Delta A(t) = \sum_{i=1}^{N} A_i exp\left(-t/\tau_i\right) \qquad (1)$$

where $t$ is the probe delay time, $A_i$ and $\tau_i$ are amplitudes of TA and decay lifetimes, respectively. Here, the number of components ($N$) to satisfactorily fit the experimental data is 2. The average lifetime ($\tau_{ave}$) was estimated from the fitting parameters according to the following equation.

$$\tau_{ave} = \sum_{i=1}^{2} A_i\tau_i^2/A_i\tau_i \qquad (2)$$

**Note S2.** Calculation of trap-assisted recombination rate coefficient.

Equation S3 shows the evolution of carrier density after pump excitation.

$$-\frac{dN(t)}{dt} = k_1 N + k_2 N^2 \qquad (3)$$

where $N(t)$ is the carrier density; $k_1$ is the monomolecular recombination rate coefficient at low carrier density; $k_2$ is the bimolecular recombination rate coefficient at high carrier density. Herein, we only focus on $k_1$ because trap-assisted recombination is one of monomolecular recombination. Thus, we can simplify the Equation S3 as follows:

$$-\frac{dN(t)}{dt} = k_1 N \qquad (4)$$

For further adjustment,

$$\frac{dN(t)}{N} = -k_1 dt \qquad (5)$$

Integrate both sides of the Equation S5 at the same time.

$$\int_0^N \frac{dN}{N} = -k_1 \int_0^t dt \qquad (6)$$

Then,

$$lnN = -k_1 t + C \qquad (7)$$

Where $C$ is a constant. When $t = 0$, $N = N_0$ ($N_0$ is the initial carrier density). Thus, $C = \ln N_0$.

Half-lifetime ($t_{1/2}$) is generally used for first-order decay process. Suppose that when $N_0$ decays to half, $t = t_{1/2}$,

$$ln\frac{1}{2}N_0 = -k_1 t_{1/2} + lnN_0 \qquad (8)$$

Therefore,

$$t_{1/2} = \frac{ln2}{k_1} \qquad (9)$$

Changing the excitation intensity will vary the initial carrier density. Since $k_1$ is the intrinsic decay rate constant, the time for the initial carrier density decaying to half ($t_{1/2}$) is fixed, thus the decay curve of free electron-hole recombination remains unchanged and independent of excitation intensity.

If trap-assisted recombination of electrons and holes occurs, we assume that holes are trapped firstly and then recombine with electrons. In this case, we denote $N_{TH}$ and $N_{FH}$ as density of trapped and free holes, respectively; $N_{TE}$ and $N_{FE}$ as density of electrons bound to trapped holes and free electrons, respectively; $k_{TH}$ as intrinsic trapping rate constant of holes and $k_{TE}$ as trapping rate constant of electrons captured by pre-trapped holes; $N_0$ as the initial carrier density; $t_{TH}$ as hole capture time and $t_{TE}$ as electron capture time. Since the holes are trapped at first, we have following equations.

$$\frac{dN_{TH}}{dt} = N_{FH} k_{TH} = (N_0 - N_{TH}) k_{TH} \qquad (10)$$

Integrate both sides of Equation S10 at the same time.

$$\int_0^N \frac{dN_{TH}}{N_0 - N_{TH}} = k_{TH} \int_0^{t_{TH}} dt \qquad (11)$$

According to the integration result, when $N = N_{TH}$,

$$ln\left(1 - \frac{N_{TH}}{N_0}\right) = -k_{TH}t_{TH} \quad (12)$$

The trapped holes then continue to attract free electrons,

$$\frac{dN_{TE}}{dt} = N_{FE}(N_{TH} - N_{TE})k_{TE} \approx (N_{TH} - N_{TE})k_{TE} \quad (13)$$

Integrate both sides of Equation S13 at the same time.

$$\int_0^N \frac{dN_{TE}}{N_{TH} - N_{TE}} = k_{TE}\int_0^{t_{TE}} dt \quad (14)$$

According to the integration result, when $N = N_{TE}$,

$$ln\left(1 - \frac{N_{TE}}{N_{TH}}\right) = -k_{TE}t_{TE} \quad (15)$$

It can be seen that the $t_{TE}$ is related to $N_{TH}$. When the $N_{TH}$ increases, the electron capture rate increases, and the recombination rate of electrons and holes increases, thus the dynamic decay accelerates. The variability of excitation intensity will change the $N_0$, which in turn influences the $N_{TH}$ and carrier capture time $t_{TE}$, leading to different decay curves.

Reference

1 L. A. Baker, S. E. Greenough and V. G. Stavros, *J. Phys. Chem. Lett.*, 2016, **7**, 4655-4665.